Quantifying heat-related mortality attributable to human-induced climate change

Rupert Stuart-Smith (✉ rupert.stuart-smith@ouce.ox.ac.uk)
Oxford Sustainable Law Programme, University of Oxford https://orcid.org/0000-0002-1854-0641
Ana Vicedo-Cabrera
Sihan Li
Friederike Otto
Kristine Belesova
Andy Haines
Luke Harrington
Jeremy Hess
Rashmi Venkatraman
Thom Wetzer
Alistair Woodward
Kristie Ebi

Research Article

Keywords: Climate change, attribution, health, epidemiology

Posted Date: March 17th, 2023

DOI: https://doi.org/10.21203/rs.3.rs-2702337/v1

Quantifying heat-related mortality attributable to human-induced climate change

Authors

Rupert F. Stuart-Smith[1,2,3*], Ana M. Vicedo-Cabrera[4,5], Sihan Li[2,6,7], Friederike E.L. Otto[2,8], Kristine Belesova[9], Andy Haines[10,11], Luke J. Harrington[12], Jeremy J. Hess[13], Rashmi Venkatraman[10,11], Thom Wetzer[2,3,14], Alistair Woodward[15], & Kristie L. Ebi[16]

Affiliations

[1] Environmental Change Institute, University of Oxford, Oxford, OX1 3QY, UK

[2] Oxford Sustainable Law Programme, University of Oxford, Oxford, OX1 3QY, UK

[3] Smith School of Enterprise and the Environment, University of Oxford, Oxford, OX1 3QY, UK

[4] Institute of Social and Preventive Medicine, University of Bern, Bern, Switzerland

[5] Oeschger Center for Climate Change Research, University of Bern, Bern, Switzerland

[6] School of Geography and the Environment, University of Oxford, Oxford, OX1 3QY, UK

[7] Department of Geography, University of Sheffield, Sheffield, UK, S3 7ND

[8] The Grantham Institute for Climate Change, Imperial College London, London, SW7 2AZ, UK

[9] Department of Primary Care & Public Health, School of Public Health, Imperial College London, London, W6 8RP

[10] Centre on Climate Change and Planetary Health, London School of Hygiene & Tropical Medicine, London, WC1H 9SH, UK

[11] Department of Public Health, Environments and Society, London School of Hygiene & Tropical Medicine, London, WC1H 9SH, UK

[12] Te Aka Mātuatua School of Science, University of Waikato, Hillcrest, Hamilton 3216, New Zealand.

[13] Department of Environmental and Occupational Health Sciences, University of Washington, Seattle, Washington, 98195, USA

[14] Faculty of Law, University of Oxford, Oxford, OX1 3UL, UK

[15] Section of Epidemiology and Biostatistics, School of Population Health, University of Auckland, Auckland 1010, New Zealand

[16] Department of Global Health, University of Washington, Seattle, Washington, 98195, USA

*Corresponding author. Email: rupert.stuart-smith@ouce.ox.ac.uk

Abstract

The impacts of anthropogenic climate change remain largely unquantified. Here we detail and address limitations in existing methods for attributing health impacts to climate change, including the representation of the climate-health relationship, choices in calculating counterfactual temperatures, assessment of long-term trends and individual events, and estimation of the effects of adaptation. Applying these methods, we found over 1,700 deaths attributable to anthropogenic temperature increases in the Canton of Zürich (Switzerland) over 50 years. Changing exposures and vulnerabilities to heat, including due to adaptation, avoided over 700 deaths. Heat-related deaths peak during heatwaves but also occur throughout summer months and the fraction of deaths attributable to climate change is higher outside heatwaves. Our approach supports targeted adaptation measures, and the analyses described here could be adapted and applied elsewhere to assess the effect of climate change on other health impacts or economic losses.

Teaser

Synthesis of climatological and epidemiology methods finds 1,700 heat deaths attributable to climate change in the Canton of Zürich (1969-2018).

MAIN TEXT

Introduction

Human-induced climate change causes substantial morbidity and mortality from increasingly frequent and intense extreme weather events, rising temperatures and sea levels, and altered seasonality (*1*, *2*). These changes have direct physiological effects, shift the distribution of pathogens and disease vectors, reduce the yields and nutrient quality of food crops, and influence socioeconomic determinants of health. As global temperatures rise, the magnitude of associated health impacts is projected to increase further (*3–5*). Studies quantifying the already-occurring effects of climate change on health can improve awareness of its impacts, inform adaptation decisions and political negotiations around loss and damage (*6*), and provide evidence for climate-related lawsuits (*7*), but remain limited in number, scope, regional coverage, and in the rigour of methods applied. No previous paper describes methods for attributing health impacts to climate change comprehensively, including the synthesis of climate attribution and epidemiological approaches. Here, we develop an approach for quantifying climate change effects on heat-related mortality in a specific location. Methods described in this article can be adapted to assess effects of climate change on other health impacts or in other regions.

Widely-applied methods exist for quantifying the effect of climate change on weather (*8*) and climatic conditions on health (*9*, *10*). Recent studies extended attribution analyses from assessing climate change influence on meteorological events to their economic and health impacts, including on heat-related mortality (*10–13*). However, estimating the effect of climate change on current or historical health impacts is not a trivial task. Several methodological questions arise that have not yet been addressed sufficiently. These include how the climate-health relationship affects the approach for quantifying climate change impacts, how to account for adaptation and the various sources of uncertainty stemming from climate-science and epidemiological components of analyses, and what methods are best to quantify impacts resulting from single events and effects accumulated over longer periods of time.

We present a case study of the effect of climate change on observed heat-mortality impacts in the canton of Zürich (Switzerland) over 1969-2018 to illustrate method-related issues, and we argue that combining state-of-the-art climate-science and epidemiological methods can address the

limitations of the approaches most commonly used at present. We use time-varying exposure-response associations to quantify the effects of adaptation in reducing populations' exposure to heat and conduct analyses that compare heat-related mortality attributable to climate change within and outside of heatwaves.

Probability and intensity-based approaches for health attribution

Climate change attribution studies quantify the effect of anthropogenic climate change on a meteorological event or trend in a climate variable relative to a counterfactual climate in which human influence is excluded. This counterfactual climate can be represented in multiple ways. One option is to quantify the relative likelihoods that an event greater than a threshold magnitude would occur in the present and counterfactual climates. Studies also assess how much less/more intense an event of observed probability would have been without climate change, as we do here. These choices affect the representation of the climate-health relationship and the interpretation of the findings.

Probability-based assessments quantify the relative chance of exceeding a threshold magnitude with and without climate change. In practice, this approach represents the relative probabilities of the 'class of events' that meet or exceed the observed event's magnitude, rather than the specific event that occurred (*14*). Such assessments also dichotomise exposure-response relationships: impacts are considered to occur at or beyond a threshold value and those that occur below the threshold are implicitly disregarded. Furthermore, because probabilities attributable to climate change reflect temperatures at least as high as the observed, probabilistic assessments represent the effect of climate change on more severe impacts than those that occurred (*14*). However, temperature-mortality relationships are continuous above the minimum-mortality temperature, and heat-related deaths increase non-linearly with progressively higher temperatures. The overall mortality burden of moderate temperatures may be substantial since moderate temperatures occur commonly (Figure 1c).

If a study seeks to assess whether *any* heat-related deaths occur, the minimum-mortality temperature could be used as a threshold for a probability-based analysis, as is done in the epidemiological literature (*15*). Otherwise, the effect of climate change can be assessed more accurately by comparing heat-related mortality under present-climate conditions and counterfactual temperatures using the state-of-the-art methods in climate epidemiology that account for the complexity (i.e., non-linearity and delayed effects) of the temperature-mortality relationship (time-series analysis, Methods, Figure 1a). We adopted this approach here.

The intensity-based approach for attribution raises the question of how to estimate counterfactual temperatures. Previous research used bias-corrected climate-model (GCM) data to represent the historical climate, with anthropogenic and natural forcings, and a 'historical-natural' climate from which anthropogenic climate forcings are excluded (*10*). However, day-to-day variability in GCM data does not align well with observed temperatures: days with highest temperatures differ between GCMs and observations (Figure S1). Consequently, in previous studies (*10*) it was more appropriate to use mean mortality by day of the year, as done in health impact projection studies (*9*), rather than observed data as the denominator to derive the daily heat-attributable fraction of deaths (*10*). Mean values by day of the year retain seasonal patterns but do not represent the full variability of heat-related mortality. Peaks and troughs in daily mortality do not appear in averaged data.

We resolve this limitation by using observed temperatures to quantify heat-related mortality in the historical period and derive counterfactual temperatures by subtracting the anthropogenic temperature change for each day from the observations, based on climate-model and observation-based datasets. This approach is similar to that previously applied (with annual data) to quantify economic impacts of climate change (*16*). The attributable temperature change corresponds to the

difference between factual and natural temperatures with return times equal to the observations, from daily GCM and reanalysis (observation-based gridded climate data) outputs (Methods). Because the observed pattern of daily temperatures is preserved, it is appropriate to use observed daily mortality to assess heat-related deaths. This approach accords greater confidence in calculating absolute values of heat-related mortality attributable to climate change, especially during heatwave periods.

Results

Heat-related mortality attributable to anthropogenic climate change in Zürich between 1969-2018

We calculated climate-change-attributable heat-related mortality for the Canton of Zürich (Switzerland, population 1.5 million in 2021 (*17*)) over 1969-2018 as the difference between that associated with observed and counterfactual temperatures (Methods). This requires daily temperatures under factual and counterfactual conditions, daily total mortality, and the exposure-response relationship between temperature and mortality risk.

To generate counterfactual temperatures, we calculated the quantiles of daily-mean temperature frequencies in station observations from Zürich for June – August 1969-2018, the period for which mortality data were available, fitted to a logistic distribution (Methods). For each day, we calculated the temperatures under historical (factual) and counterfactual conditions with return times equal to that calculated from the observations. To do so, we fitted daily-mean temperatures for the grid cell containing the Canton of Zürich from factual and counterfactual timeseries from an ensemble of models from the Coupled Model Intercomparison Project Phase 6 (CMIP6, Table S1) and observation-based datasets (reanalysis and station observations) to a logistic distribution. In models for which historical-natural simulations were unavailable, and for the observation-based data we applied a widely-used regression-based method for generating counterfactual temperatures (*8*) (Methods).

Daily counterfactual data were calculated by subtracting from station observations a temperature anomaly attributable to anthropogenic climate change, equal to the difference between factual and counterfactual temperatures in each model and observation-based dataset. Summer (June-August) warming attributable to anthropogenic influence increased across the study period, reaching 1-1.5 °C in 2009-2018 in model simulations, and slightly higher in reanalysis datasets (Figure S2).

The effect of ambient temperature on mortality is characterised by location-specific exposure-response associations (*18*). We calculated the exposure-response association between observed temperature and all-cause mortality using an approach applied to assess past and projected relationships between temperature and mortality risk in a range of settings (*10*, *19*, *20*) (Figure 1a). We applied a distributed lag non-linear model to account for the non-linearity of the association and potential mortality displacement effect up to 7 days of lag (Methods). We used this association to estimate the temperature-attributable fraction of excess mortality, and calculated heat-related mortality for each day when temperatures exceeded the minimum-mortality temperature. Heat-related mortality was quantified using observed mortality for each day and the relative risk corresponding to the daily temperature.

Between 1969-2018, 6,217 (2,825-9,623, 5-95% empirical confidence interval) heat-related deaths occurred in the Canton of Zürich. In the counterfactual scenarios, heat-related mortality is 4,457 (synthesis value of model and observed datasets, 1046-8051), leaving 1,712 (276-3,329) deaths attributable to anthropogenic climate change (Table S3). This is equal to 27.5% of heat-related mortality and 1.4% (0.2-2.8%) of summer all-cause mortality in Zürich over this period (Figure 2b). Results by model and synthesis series are provided in Tables S3 and S4.

Previous research found that globally 0.6% of warm-season all-cause mortality (37% of heat-related mortality) was attributable to anthropogenic climate change over 1991-2018 (0.74% and 31.3% respectively for Switzerland) (*10*). Here, heat-related mortality attributable to climate change was calculated as the difference between growing numbers of heat-related deaths occurring at increasingly common high temperatures and reduced numbers of deaths occurring at decreasingly common moderate temperatures (the difference between the areas under the curves in Figure 1c). Our results show that the proportion of all-cause mortality attributed to anthropogenic increases in temperatures rises as attributable warming increases (Figure 2c).

Trend attribution and accounting for adaptation

Our results find a substantial burden of heat-related mortality attributable to climate change. As in previous studies, we used a single exposure-response relationship derived from all observed mortality and temperature series representing the average vulnerability across the study period (*10*). Using the full timeseries reduces uncertainty in the exposure-response association, especially in locations with a low number of observations. However, the temperature-mortality relationship evolves over time due to changes in demographic (*21*), physiological, behavioural, socioeconomic, and infrastructural factors (*22*). A long daily-mortality dataset allows the use of a subset of the study period to assess changes in exposure-response associations over time. We use these changes to estimate the effect of adaptation on heat-related mortality by dividing all-cause summer mortality into three subsets: 1969-1985, 1986-2003, and 2004-2018 and derived exposure-response associations expressed as relative risk (relative to the minimum-mortality temperature) for each period using daily-mean temperature observations (Figure S3).

We compared results obtained using a single (full-period) and time-varying exposure-response associations. Across the full analysis period, heat-related mortality attributable to climate change was 1.4% of all-cause mortality with both time-varying and constant exposure-response associations, supporting previous approaches (*10*). However, using a constant exposure-response association underestimates heat-related mortality at the start of the timeseries, when the relationship between temperature and mortality risk is steeper, and overestimates heat-related mortality in the period since 2004, as risk was reduced due to adaptation, as detailed below (Figure 2a, Figure S3).

We quantify the effects of changing exposure and vulnerability of populations by using time-varying exposure-response associations to compare mortality in scenarios in which the exposure-response relationship derived for 1986-2003 is applied to 2004-2018 ('no adaptation') and in which the relationship is recalculated based on observed temperature and mortality over the period 2004-2018 ('adaptation'). In the 'adaptation' scenario, the exposure-response relationship reflects the changed sensitivity of the population to high temperatures over time. This could represent effects of changes in demographics, public health and healthcare systems, physiological adaptation, behaviour, access to blue and green spaces, and infrastructure. Our approach does not facilitate disaggregation of effects of specific measures. The Canton of Zürich has implemented limited measures for reducing heat impacts beyond those introduced at the Federal level (*23*), including information campaigns advising vulnerable populations on safe behaviour during heatwaves (*24*). Because population ageing in Zürich has increased vulnerability to heat (*21*), decreases in the overall sensitivity of mortality to temperature are explained by adaptation-like changes irrespective of whether they constitute explicit responses to heat. We refer to these changes as 'adaptation'.

Under the 'no adaptation' scenario, in which these changes do not take place, an additional 738 deaths occurred over 1969-2018, relative to the 'adaptation' scenario when, in each case, mortality was calculated based on observed temperatures. The change in the exposure-response relationship from 2004 onwards thus caused a 11% reduction in mortality over the period 2004-

2018 relative to the mortality expected in the absence of these changes (Table S5). In both adaptation and no-adaptation scenarios, heat-related mortality attributable to climate change rose throughout the study period, with adaptation limiting this increase (Table 1, Figure 2c).

Our results suggest that, at least for Zürich, adaptation can reduce the burden of mortality associated with high temperatures. These results contrast with previous research that compared exposure-response associations for successive periods of time to evaluate England's heatwave plan and found very little change in the temperature-risk relationship following its introduction (*25*). Nevertheless, substantial climate-change-attributable heat-related mortality continues to occur in Zürich. Under both 'adaptation' and 'no-adaptation' scenarios, attributable heat-related mortality constitutes an increasing portion of all-cause summer mortality at higher levels of regional warming (Figure 2c).

Attributable mortality within and outside heatwave periods

Previously-published methods could quantify heat-related mortality during heatwave periods alone (*11*, *26*), across full summers (*12*) or assess climate trends over extended periods (*10*). Probability-based assessments of heat-related mortality described above are applied to quantify impacts of climate change on heat-related mortality during events of limited duration. Our approach to estimating counterfactual temperatures provides fungible results for both periods of extreme conditions and long-term analysis allowing long-term trend attribution to be aligned with an event attribution framework. This allows us to quantify the relative portion of heat-related mortality attributable to anthropogenic climate change within and outside of heatwave periods.

We apply this approach to Zürich. To assess heat-related mortality within and outside of heatwaves, we limited our analysis to the summer of 2018 and quantified heat-related mortality based on observed and counterfactual temperatures. Existing research found that human influence increased the intensity and likelihood of different aspects of the summer 2018 heatwave in Europe (*27*, *28*).

Across the summer of 2018, we estimate that 86 (55-114, 5-95% empirical confidence intervals) of 208 (114-304, 5-95% empirical confidence intervals) heat-related deaths in the Canton of Zürich are attributed to anthropogenically-driven temperature rise (i.e., 41%), based on the temperature-mortality relationship derived for 2004-2018. We define the heatwave period as 29 July – 10 August, the period of highest temperatures. Across these 12 days (13% of summer), 83 (46-115) heat-related deaths occurred, with 22 (-3-46) attributable to climate change (27% of heat-related deaths, Figure 3).

Because the temperature-mortality relationship is steepest at high temperatures, absolute values of climate-change-attributable heat-related mortality are highest on the hottest days. However, on days that are cooler but still above the minimum mortality temperature, climate change accounts for a larger proportion of the difference between the observed and minimum-mortality temperature than on hot days, and therefore a higher proportion of heat-related deaths. Our findings provide an empirical demonstration that climate change increases heat-related mortality on almost all summer days, and that while mortality peaks during heatwaves, heat-related mortality attributable to climate change also occurs outside of heatwaves.

Discussion

Our climatological and epidemiological analyses yield three main findings. First, in the Canton of Zürich, 1,712 summer heat-related deaths were attributed to anthropogenic climate change in 1969-2018. Previous research found that 90% of victims of heat-related mortality in Switzerland were 80 years old or older (*21*). Second, temperature-mortality relationships were sensitive to

adaptation. As daily temperatures increase, adaptation counteracted some heat impacts. Zürich enjoys advantages in its capacity to adapt to heat effects over many heat-exposed locations worldwide due to housing quality, high-quality health and social services, and economic prosperity. Nevertheless, substantial heat impacts were still observed. Empirical evidence for the effectiveness of adaptation is limited (*29*). The results above provide improved understanding of the effectiveness of adaptation that could support policy and practice in future. Implementing adaptation measures may incur costs in addition to the benefits detailed here, although these were beyond the scope of our analysis.

Third, heat-related mortality occurs at highest rates at the hottest temperatures. However, outside of heatwaves, the proportion of summer mortality attributable to anthropogenic climate change is higher (27% during the heatwave, versus 41% across summer 2018): climate change amplifies mortality throughout warm seasons. Analyses that focus on heatwaves alone will not capture the full effect of anthropogenic climate change on heat-related deaths.

We found that an average of 19 heat-related deaths attributable to anthropogenic climate change occurred each summer in 1969-1985, rising to 48 per summer since 2004. A simple method for allocating contributions to impacts that is commonly used in legal settings is the 'market-share approach' that estimates individual entities' contributions to losses as the product of the entity's proportional contribution to greenhouse gas emissions and the magnitude of the attributable impact (*7*). Applying this approach here indicates that cumulative greenhouse gas emissions of each of the top six highest-emitting investor and state-owned companies (*30*) caused, on average, at least one additional death per summer in Zürich since 2004 (estimates for 1969-2018 are provided in Table S6). Similar findings would be expected for many other locations worldwide.

To conduct these analyses, we refined approaches for attributing health impacts to climate change and explained that probability and intensity-based framings have different application depending on the relationship between climatic hazards and their impacts. While the method described here does not require additional data relative to the approach described in ref. (*10*), our analyses require data that are not available worldwide, including daily all-cause mortality and temperature observations. Limited availability and quality of granular health data and long-term climate observations present challenges for deriving location-specific relationships between climate variables and health outcomes, or in evaluating human influence on these climate variables.

Our results are consistent with previous analyses (*10*), demonstrate the scale of impacts already occurring because of observed climate change, and indicate the risk of worsening impacts under further warming, with global implications. The approach described can be applied elsewhere or adapted to evaluate the effect of climate change on other health risks. The methods employed here could be adapted to make greater use of reanalysis data in lieu of direct meteorological observations and estimating exposure-response associations based on available health data in conjunction with socioeconomic, institutional, climatological, demographic, and environmental information. These alterations could support evidence-based adaptation to climate change impacts on health, which disproportionately affect vulnerable groups, such as those living in poverty and urban areas (*31*). These methods could also be refined to assess the effect of climate change on other health or economic impacts.

Materials and Methods

Experimental Design

Climatological analysis

Methodological choices for climate change impact attribution. Meteorological attribution studies typically assess both the change in intensity attributable to human-influence on the climate for an event of given probability, or the change in probability of exceeding a threshold value. Previous studies assessed the health or economic impacts of climate change as the product of total impacts (for instance, heat-related deaths) and the fraction of the event likelihood (referred to as the 'Fraction of Attributable Risk', or 'FAR') for which anthropogenic climate change is responsible (*12*, *13*, *32*, *33*). FAR quantifies the portion of the probability of exceeding a threshold event magnitude that is attributable to anthropogenic climate change. As such, FAR may effectively quantify the effects of climate change when there is a threshold in the impact magnitude such that below-threshold climate hazards do not cause impacts.

However, as noted in the main text, if impacts increase continuously with the magnitude of the hazard, FAR-based assessments do not capture the effect of climate change on impacts occurring below the chosen threshold. Earlier, we explain that above the optimum, or minimum-mortality, temperature, heat-related mortality increases at progressively higher temperatures (*10*). Therefore, quantifying the attributable mortality as the difference between mortality associated with observed temperatures and the temperatures that would have occurred in the absence of climate change most accurately captures the effects of climate change on heat-related mortality.

Constructing the counterfactual temperatures. To derive the counterfactual temperature timeseries, we applied the extreme event attribution framework described in refs (*8*, *34*). The objective was to calculate the change in daily-mean temperature attributable to anthropogenic climate change for each day of the study period and subtract these values from observed temperatures, generating a counterfactual timeseries.

For each day of the study period, we calculated the return time of the temperatures in the observations. We do so by first detrending the observed temperatures by regressing against 4-yr smoothed global-mean surface temperature (GMST) using the NASA-GISS temperature dataset (*35*). We then fitted the detrended temperatures to logistic distribution that represent the distribution of temperatures in the 30-year period centred on the year in question, or for data near the end of the timeseries, the longest period that could be centred on the day in question. This ensures that the estimated return times of daily temperatures are consistent with the climate in which they occurred. We note that years near the end of the timeseries will be more affected by internal variability due to the shorter period used to estimate the mean of the temperature distribution.

The logistic distribution was chosen by fitting the detrended observed daily-mean temperatures with seasonal cycle removed (by subtracting the 30-day moving mean) to commonly used statistical distributions and applying the Anderson-Darling and Kolmogorov-Smirnov tests to identify the distribution that gave the best fit to the data. The statistical distributions attempted were the Generalised Extreme Value (GEV), Logistic, Normal, Rayleigh, and t Location Scale distributions. The seasonal cycle was reinstated through the use of observations for the factual and in constructing the counterfactual temperatures.

We then calculated the change in daily-mean temperature attributable to anthropogenic climate change as the difference between the modelled daily-mean temperatures in the present (1989-2018) and counterfactual climates ($\bar{T}_{nat}$) in climate-model and observation-based (reanalysis) simulations. The temperatures under historical and historical-natural conditions were estimated as the temperatures with the same return time as the temperature of the same day in the observations. Model and reanalysis temperatures are taken from the grid cell containing Zürich;

for the model temperatures, these are taken from an 18-member ensemble of CMIP6 models detailed in Table S1. First, the difference in temperature caused by the difference between the mean elevation of the model grid cell and the station observations is corrected for using a lapse rate of -6.5 °C km^{-1}, consistent with summer lapse rates found elsewhere in the European Alps (*36*, *37*). We then detrended the model and observation-based temperatures by regressing against each model's GMST and fit the resulting timeseries to the same statistical distribution as the observations. The distribution was shifted over time such that it reflected the temperatures of the 30-year period centred on the year in question.

We evaluated the models to assess whether the statistics of extreme heat in the models were consistent with those in the observations by comparing the scale and shape parameters of each of the model fits with that of the observations. Following ref. (*8*), the models for which the 5-95% confidence intervals of these parameters of the statistical fits overlapped with the 5-95% confidence intervals of the parameters of the observations, were initially selected for use in the analysis. Since only one model passed this evaluation step, and it is preferable to include multiple models to better account for systematic uncertainty in the model representation of the climate system, due to model structural biases and differing representations of physical processes, we expanded the range of parameter values used to evaluate models slightly (by 5% relative to the 5 and 95% confidence intervals). This increased the number of models passing the evaluation step to seven. All seven selected models produce warming attributable to human influence that, at the end of the series lie within the range of the observation-based datasets (Figure S2).

We then calculated the attributable change in temperature for each day of the heatwave in all models that pass the evaluation step. We used the CMIP6-model ensemble to simulate the distribution of daily temperatures in the historical period and in the absence of anthropogenic greenhouse-gas and aerosol emissions. We used daily output from historical (1850-2014) and SSP 5-8.5 (2015-2050) runs as transient simulations. For models for which both transient and historical-natural simulations (from the Detection and Attribution Model Intercomparison Project, DAMIP (*38*)) were available, the attributable change in temperature was calculated as the difference between the temperatures in the two sets of simulations, for return times equal to those in the observations. The return times of model temperatures were calculated using the same approach taken for the observations, with return times calculated based on a distribution representing the 30-year period centred on the year in question.

For the models for which historical-natural simulations were unavailable, the transient simulations were used and the distribution of daily-mean temperatures in the absence of human influence estimated by shifting the mean of the temperature distribution by the product of the change in GMST attributable to anthropogenic climate influence and a scaling factor. Global-mean human-induced warming is taken from the Global Warming Index, an estimate of the anthropogenic contribution to global externally-forced temperature change (*39*). The scaling factor is dataset and region-specific and is the regression co-efficient (α) calculated in detrending the model/observational temperature data, which is the ratio between the gradients of local temperature observations and (4-yr smoothed) GMST from NASA-GISS (*35*) $\left(\alpha = \frac{dT_{obs}/dt}{dT_{GMST}/dt}\right)$. The same approach was also applied to the station observations and three climate reanalysis datasets: the Modern-Era Retrospective analysis for Research and Applications, Version 2 (MERRA-2) (*40*), Berkeley Earth Surface Temperature Project (*41*), and ERA5 (*42*, *43*). These two methods for calculating counterfactual temperatures are both commonly used in attribution studies when historical-natural simulations are available for some models but not others (*8*).

The regression-based method used for timeseries for which historical-natural simulations were unavailable can effectively account for the effect of anthropogenic influence on the climate on multi-decadal to centennial scales, it does not account for interdecadal variability. Consequently, this approach does not capture short-term influences on region-specific warming, such as lowered central European temperatures in the 1970s due to anthropogenic aerosol emissions (*44*, *45*) and so may overestimate temperature anomalies attributable to anthropogenic influence in this period, as seen in Figure S2.

This approach is also based on two assumptions. First, using GMST as a covariate to represent anthropogenic influence on local temperatures assumes that the long-term proportional contributions of anthropogenic and natural forcing to temperature change are equal at local and global scales, and therefore that there are no independent local factors that could create century-scale local climate trends. Such factors might plausibly include local changes in albedo due to land-cover alterations over the past 150 years. This is a widely-applied assumption in climate change attribution studies (*8*). Therefore, we adopt this assumption here. Second, a common assumption in climate change attribution studies is that the trend in temperature extremes shifts with GMST, and that the scale parameter of the temperature distribution is unchanged over time. This is well supported for studies using large ensembles of model simulations (*8*). Nevertheless, we tested this assumption by evaluating the sensitivity of attributable mortality to the values of the scale parameter. We iteratively fit 30-yr windows of detrended data to the statistical distribution and found that mortality is unchanged (<0.01% change) for a 1 standard deviation shift in the values of the parameters.

Epidemiological analysis

Our epidemiological analysis largely replicates the approach applied by Vicedo-Cabrera et al. (2021) (*10*) where the methods are described in full, with an important methodological adaptation. Instead of calculating mortality based on factual and counterfactual climate-model simulations, and mean mortality for each day of the warm season, we calculated heat-related mortality based on observed (summer) mortality and temperatures. This gives greater confidence in our estimation of absolute values of heat-related mortality (Table S3) and allows us to account for changes in population. The values in Table S4 show the proportion of all-cause summer mortality attributable to the impact of anthropogenic climate change on summer temperatures, and are therefore unaffected by population change. We calculated counterfactual mortality using the counterfactual temperatures generated as described in the climatological analysis section, above.

Here we provide a brief overview of the epidemiological methods applied, noting elements of the methods specific to our study. We estimated the temperature-mortality relationship by conducting a time-series analysis with generalised linear models and quasi-Poisson regression using observed daily-mean temperature and mortality data during summer months (June-August)(*10*). We modelled the temperature-mortality dependency with a distributed lag non-linear model that simultaneously accounts for delayed effects and non-linearity of the association, typically found in temperature-health studies. Specifically, the exposure-response dimension was defined with a natural spline with two internal knots placed in the 50th and 90th percentile of the summer temperature distribution. The lag-response dimension also included a natural spline with two internal knots equally spaced in the log scale and up to 7 days of lag. The time-series model included a natural spline of day of the year with 4 degrees of freedom and an interaction by year, and a natural spline of time with 1 knot every 10 years to control for both seasonality and long-term trends. The specifications of the time series model and the definition of the cross-basis function of temperature are the ones described in Vicedo-Cabrera et al. (2021) and

have been extensively used in previous assessments (*10*, *15*, *46*, *47*). We did not control for air pollution and/or humidity since previous assessments suggested that the role of these variables as confounders was negligible (*15*, *48*). The analysis was performed across the whole study period (June-August 1969-2018) to obtain the overall temperature-mortality association, and by subperiod to obtain the corresponding association estimates.

We quantified the mortality attributed to heat using the observed mortality and the risk estimate corresponding to the mean temperature each day, for the observed and counterfactual series, using the method described elsewhere (*49*). Previous epidemiological research showed that deriving such associations using time-series analysis of daily-mean temperatures and daily all-cause mortality effectively describes climatic influence on mortality (*15*, *50*). We then sum the daily temperature-related deaths of the days when mean temperature (both in the observed and counterfactual series) was above the temperature of minimum mortality (i.e., temperature value for which the mortality risk is minimum). In doing so, we considered the risk contribution of the preceding 7 days, following findings that the effect of heat on mortality lasts for up to a week (*24*, *51*). We derived ensemble estimates for the counterfactual scenario as the average across mortality in each counterfactual temperature timeseries. We quantified the uncertainty of the estimates by generating 1,000 samples of the coefficients defining the exposure-response association through Monte Carlo simulations, assuming a multivariate normal distribution. We derived the 95% empirical confidence intervals (eCI) from the resulting distribution, corresponding to the 2.5th and 97.5th percentiles. The eCI of the ensemble estimates of the counterfactual scenarios (i.e., by averaging across the single-series estimates) were estimated by combining the single-series distributions. Thus, in this way we account for both uncertainty of the exposure-response function and the variability across the different counterfactual series.

The mortality attributable to human influence is then quantified as the difference between the observed mortality due to heat (i.e., using the data from station observations) and the corresponding burden estimated with the counterfactual series. The computation was performed across the whole study period, by subperiods and during summer 2018 and the 12 days of the heatwave in that summer. Daily-mean temperature is widely used as a determinant of heat exposure in calculating temperature-mortality relationships (*9*, *10*, *15*, *52*).

References

1. M. Romanello, C. di Napoli, P. Drummond, C. Green, H. Kennard, P. Lampard, D. Scamman, N. Arnell, S. Ayeb-Karlsson, L. B. Ford, K. Belesova, K. Bowen, W. Cai, M. Callaghan, D. Campbell-Lendrum, J. Chambers, K. R. van Daalen, C. Dalin, N. Dasandi, S. Dasgupta, M. Davies, P. Dominguez-Salas, R. Dubrow, K. L. Ebi, M. Eckelman, P. Ekins, L. E. Escobar, L. Georgeson, H. Graham, S. H. Gunther, I. Hamilton, Y. Hang, R. Hänninen, S. Hartinger, K. He, J. J. Hess, S.-C. Hsu, S. Jankin, L. Jamart, O. Jay, I. Kelman, G. Kiesewetter, P. Kinney, T. Kjellstrom, D. Kniveton, J. K. W. Lee, B. Lemke, Y. Liu, Z. Liu, M. Lott, M. L. Batista, R. Lowe, F. MacGuire, M. O. Sewe, J. Martinez-Urtaza, M. Maslin, L. McAllister, A. McGushin, C. McMichael, Z. Mi, J. Milner, K. Minor, J. C. Minx, N. Mohajeri, M. Moradi-Lakeh, K. Morrissey, S. Munzert, K. A. Murray, T. Neville, M. Nilsson, N. Obradovich, M. B. O'Hare, T. Oreszczyn, M. Otto, F. Owfi, O. Pearman, M. Rabbaniha, E. J. Z. Robinson, J. Rocklöv, R. N. Salas, J. C. Semenza, J. D. Sherman, L. Shi, J. Shumake-Guillemot, G. Silbert, M. Sofiev, M. Springmann, J. Stowell, M. Tabatabaei, J. Taylor, J. Triñanes, F. Wagner, P. Wilkinson, M. Winning, M. Yglesias-González, S. Zhang, P. Gong, H. Montgomery, A. Costello, The 2022 report of the Lancet Countdown on health and climate change: health at the mercy of fossil fuels. *The Lancet*. **400**, 1619–1654 (2022).
2. G. Cissé, R. McLeman, H. Adams, P. Aldunce, K. Bowen, D. Campbell-Lendrum, S. Clayton, K. L. Ebi, J. Hess, C. Huang, Q. Liu, G. McGregor, J. Semenza, M. C. Tirado, "Health, Wellbeing, and the Changing Structure of Communities" in *Climate Change 2022: Impacts, Adaptation, and Vulnerability. Contribution of Working Group II to the Sixth Assessment Report of the Intergovernmental Panel on Climate Change*, H.-O. Pörtner, D. C. Roberts, M. Tignor, E. S. Poloczanska, K. Mintenbeck, A. Alegría, M. Craig, S. Langsdorf, S. Löschke, V. Möller, A. Okem, B. Rama, Eds. (Cambridge University Press, Cambridge, UK and New York, NY, USA, 2022).

3. N. Watts, M. Amann, N. Arnell, S. Ayeb-Karlsson, J. Beagley, K. Belesova, M. Boykoff, P. Byass, W. Cai, D. Campbell-Lendrum, S. Capstick, J. Chambers, S. Coleman, C. Dalin, M. Daly, N. Dasandi, S. Dasgupta, M. Davies, C. di Napoli, P. Dominguez-Salas, P. Drummond, R. Dubrow, K. L. Ebi, M. Eckelman, P. Ekins, L. E. Escobar, L. Georgeson, S. Golder, D. Grace, H. Graham, P. Haggar, I. Hamilton, S. Hartinger, J. Hess, S.-C. Hsu, N. Hughes, S. Jankin Mikhaylov, M. P. Jimenez, I. Kelman, H. Kennard, G. Kiesewetter, P. L. Kinney, T. Kjellstrom, D. Kniveton, P. Lampard, B. Lemke, Y. Liu, Z. Liu, M. Lott, R. Lowe, J. Martinez-Urtaza, M. Maslin, L. McAllister, A. McGushin, C. McMichael, J. Milner, M. Moradi-Lakeh, K. Morrissey, S. Munzert, K. A. Murray, T. Neville, M. Nilsson, M. O. Sewe, T. Oreszczyn, M. Otto, F. Owfi, O. Pearman, D. Pencheon, R. Quinn, M. Rabbaniha, E. Robinson, J. Rocklöv, M. Romanello, J. C. Semenza, J. Sherman, L. Shi, M. Springmann, M. Tabatabaei, J. Taylor, J. Triñanes, J. Shumake-Guillemot, B. Vu, P. Wilkinson, M. Winning, P. Gong, H. Montgomery, A. Costello, The 2020 report of The Lancet Countdown on health and climate change: responding to converging crises. *The Lancet*. **397**, 129–170 (2021).
4. A. Haines, K. Ebi, The Imperative for Climate Action to Protect Health. *New England Journal of Medicine*. **380**, 263–273 (2019).
5. K. L. Ebi, J. Balbus, G. Luber, A. Bole, A. R. Crimmins, G. E. Glass, S. Saha, M. M. Shimamoto, J. M. Trtanj, J. L. White-Newsome, "Human Health" in *Impacts, Risks, and Adaptation in the United States: The Fourth National Climate Assessment, Volume II*, D. R. Reidmiller, C. W. Avery, D. R. Easterling, K. E. Kunkel, K. L. M. Lewis, T. K. Maycock, B. C. Stewart, Eds. (Washington, DC, 2018; https://nca2018.globalchange.gov/chapter/14/), pp. 572–603.
6. R. A. James, R. G. Jones, E. Boyd, H. R. Young, F. E. L. Otto, C. Huggel, J. S. Fuglestvedt, "Attribution: How Is It Relevant for Loss and Damage Policy and Practice?" in *Loss and Damage from Climate Change* (Springer, Cham, 2019; http://link.springer.com/10.1007/978-3-319-72026-5_5), pp. 113–154.
7. R. F. Stuart-Smith, F. E. L. Otto, A. I. Saad, G. Lisi, P. Minnerop, K. C. Lauta, K. van Zwieten, T. Wetzer, Filling the evidentiary gap in climate litigation. *Nat Clim Chang*. **11**, 651–655 (2021).
8. S. Philip, S. Kew, G. J. van Oldenborgh, F. E. L. Otto, R. Vautard, K. van der Wiel, A. King, F. Lott, J. Arrighi, R. Singh, M. van Aalst, A protocol for probabilistic extreme event attribution analyses. *Adv Stat Climatol Meteorol Oceanogr*. **6**, 177–203 (2020).
9. A. M. Vicedo-Cabrera, F. Sera, A. Gasparrini, Hands-on Tutorial on a Modeling Framework for Projections of Climate Change Impacts on Health. *Epidemiology*. **30**, 321–329 (2019).
10. A. M. Vicedo-Cabrera, N. Scovronick, F. Sera, D. Royé, R. Schneider, A. Tobias, C. Astrom, Y. Guo, Y. Honda, D. M. Hondula, R. Abrutzky, S. Tong, M. de S. Z. S. Coelho, P. H. N. Saldiva, E. Lavigne, P. M. Correa, N. V. Ortega, H. Kan, S. Osorio, J. Kyselý, A. Urban, H. Orru, E. Indermitte, J. J. K. Jaakkola, N. Ryti, M. Pascal, A. Schneider, K. Katsouyanni, E. Samoli, F. Mayvaneh, A. Entezari, P. Goodman, A. Zeka, P. Michelozzi, F. De'Donato, M. Hashizume, B. Alahmad, M. H. Diaz, C. D. L. C. Valencia, A. Overcenco, D. Houthuijs, C. Ameling, S. Rao, F. di Ruscio, G. Carrasco-Escobar, X. Seposo, S. Silva, J. Madureira, I. H. Holobaca, S. Fratianni, F. Acquaotta, H. Kim, W. Lee, C. Iniguez, B. Forsberg, M. S. Ragettli, Y. L. L. Guo, B. Y. Chen, S. Li, B. Armstrong, A. Aleman, A. Zanobetti, J. Schwartz, T. N. Dang, D. v. Dung, N. Gillett, A. Haines, M. Mengel, V. Huber, A. Gasparrini, The burden of heat-related mortality attributable to recent human-induced climate change. *Nat Clim Chang*. **11**, 492–500 (2021).
11. D. Mitchell, Human Influences on Heat-Related Health Indicators During the 2015 Egyptian Heat Wave. *Bull Am Meteorol Soc*. **97**, S70–S74 (2016).
12. D. Mitchell, C. Heaviside, S. Vardoulakis, C. Huntingford, G. Masato, B. P Guillod, P. C. Frumhoff, A. Bowery, D. Wallom, M. R. Allen, Attributing human mortality during extreme heat waves to anthropogenic climate change. *Environmental Research Letters*. **11**, 074006 (2016).
13. B. J. Clarke, F. E. L. Otto, R. G. Jones, Inventories of extreme weather events and impacts: Implications for loss and damage from and adaptation to climate extremes. *Clim Risk Manag*. **32**, 100285 (2021).
14. S. E. Perkins-Kirkpatrick, D. A. Stone, D. M. Mitchell, S. Rosier, A. D. King, Y. T. E. Lo, J. Pastor-Paz, D. Frame, M. Wehner, On the attribution of the impacts of extreme weather events to anthropogenic climate change. *Environmental Research Letters*. **17**, 024009 (2022).
15. A. Gasparrini, Y. Guo, M. Hashizume, E. Lavigne, A. Zanobetti, J. Schwartz, A. Tobias, S. Tong, J. Rocklöv, B. Forsberg, M. Leone, M. de Sario, M. L. Bell, Y.-L. L. Guo, C. Wu, H. Kan, S.-M. Yi, M. de Sousa Zanotti Stagliorio Coelho, P. H. N. Saldiva, Y. Honda, H. Kim, B. Armstrong, Mortality risk attributable to high and low ambient temperature: a multicountry observational study. *The Lancet*. **386**, 369–375 (2015).
16. N. S. Diffenbaugh, M. Burke, Global warming has increased global economic inequality. *Proc Natl Acad Sci U S A*. **116**, 9808–9813 (2019).
17. Swiss Federal Statistical Office, Demographic balance by institutional units. *STAT-TAB* (2022).
18. A. Gasparrini, Modeling exposure–lag–response associations with distributed lag non-linear models. *Stat Med*. **33**, 881–899 (2014).
19. Y. T. E. Lo, D. M. Mitchell, R. Thompson, E. O'Connell, A. Gasparrini, Estimating heat-related mortality in near real time for national heatwave plans. *Environmental Research Letters*. **17**, 024017 (2022).
20. A. Gasparrini, Y. Guo, F. Sera, A. M. Vicedo-Cabrera, V. Huber, S. Tong, M. de Sousa Zanotti Stagliorio Coelho, P. H. Nascimento Saldiva, E. Lavigne, P. Matus Correa, N. Valdes Ortega, H. Kan, S. Osorio, J. Kyselý, A. Urban, J. J.

K. Jaakkola, N. R. I. Ryti, M. Pascal, P. G. Goodman, A. Zeka, P. Michelozzi, M. Scortichini, M. Hashizume, Y. Honda, M. Hurtado-Diaz, J. Cesar Cruz, X. Seposo, H. Kim, A. Tobias, C. Iñiguez, B. Forsberg, D. O. Åström, M. S. Ragettli, Y. L. Guo, C. Wu, A. Zanobetti, J. Schwartz, M. L. Bell, T. N. Dang, D. Do Van, C. Heaviside, S. Vardoulakis, S. Hajat, A. Haines, B. Armstrong, Projections of temperature-related excess mortality under climate change scenarios. *Lancet Planet Health*. **1**, e360–e367 (2017).

21. E. de Schrijver, M. Bundo, M. S. Ragettli, F. Sera, A. Gasparrini, O. H. Franco, A. M. Vicedo-Cabrera, Nationwide Analysis of the Heat- and Cold-Related Mortality Trends in Switzerland between 1969 and 2017: The Role of Population Aging. *Environ Health Perspect*. **130** (2022), doi:10.1289/EHP9835.
22. D. Mitchell, Climate attribution of heat mortality. *Nat Clim Chang*. **11**, 467–468 (2021).
23. M. S. Ragettli, M. Röösli, Hitzeaktionspläne zur Prävention von hitzebedingten Todesfällen – Erfahrungen aus der Schweiz. *Bundesgesundheitsblatt Gesundheitsforschung Gesundheitsschutz*. **62**, 605–611 (2019).
24. M. S. Ragettli, A. M. Vicedo-Cabrera, C. Schindler, M. Röösli, Exploring the association between heat and mortality in Switzerland between 1995 and 2013. *Environ Res*. **158**, 703–709 (2017).
25. L. Williams, B. Erens, S. Ettelt, S. Hajat, T. Manacorda, N. Mays, Evaluation of the Heatwave Plan for England Final report (2019) (available at www.piru.ac.uk).
26. Y. Guo, A. Gasparrini, S. Li, F. Sera, A. M. Vicedo-Cabrera, M. de S. Z. S. Coelho, P. H. N. Saldiva, E. Lavigne, B. Tawatsupa, K. Punnasiri, A. Overcenco, P. M. Correa, N. V. Ortega, H. Kan, S. Osorio, J. J. K. Jaakkola, N. R. I. Ryti, P. G. Goodman, A. Zeka, P. Michelozzi, M. Scortichini, M. Hashizume, Y. Honda, X. Seposo, H. Kim, A. Tobias, C. Íñiguez, B. Forsberg, D. O. Åström, Y. L. Guo, B.-Y. Chen, A. Zanobetti, J. Schwartz, T. N. Dang, D. do Van, M. L. Bell, B. Armstrong, K. L. Ebi, S. Tong, Quantifying excess deaths related to heatwaves under climate change scenarios: A multicountry time series modelling study. *PLoS Med*. **15**, e1002629 (2018).
27. D. Barriopedro, P. M. Sousa, R. M. Trigo, R. García-Herrera, A. M. Ramos, The Exceptional Iberian Heatwave of Summer 2018. *Bull Am Meteorol Soc*. **101**, S29–S34 (2020).
28. P. Yiou, J. Cattiaux, D. Faranda, N. Kadygrov, A. Jézéquel, P. Naveau, A. Ribes, Y. Robin, S. Thao, G. J. van Oldenborgh, M. Vrac, Analyses of the Northern European Summer Heatwave of 2018. *Bull Am Meteorol Soc*. **101**, S35–S40 (2020).
29. L. Berrang-Ford, A. J. Sietsma, M. Callaghan, J. C. Minx, P. F. D. Scheelbeek, N. R. Haddaway, A. Haines, A. D. Dangour, Systematic mapping of global research on climate and health: a machine learning review. *Lancet Planet Health*. **5196** (2021), doi:10.1016/S2542-5196(21)00179-0.
30. R. Heede, Tracing anthropogenic carbon dioxide and methane emissions to fossil fuel and cement producers, 1854–2010. *Clim Change*. **122**, 229–241 (2014).
31. The Lancet, 2022 heatwaves: a failure to proactively manage the risks. *The Lancet*. **400**, 407 (2022).
32. D. J. Frame, M. F. Wehner, I. Noy, S. M. Rosier, The economic costs of Hurricane Harvey attributable to climate change. *Clim Change*. **160**, 271–281 (2020).
33. D. J. Frame, S. M. Rosier, I. Noy, L. J. Harrington, T. Carey-Smith, S. N. Sparrow, D. A. Stone, S. M. Dean, Climate change attribution and the economic costs of extreme weather events: a study on damages from extreme rainfall and drought. *Clim Change*. **162**, 781–797 (2020).
34. G. J. van Oldenborgh, K. van der Wiel, S. Kew, S. Philip, F. E. L. Otto, R. Vautard, A. King, F. Lott, J. Arrighi, R. Singh, M. van Aalst, Pathways and pitfalls in extreme event attribution. *Clim Change*. **166**, 13 (2021).
35. N. J. L. Lenssen, G. A. Schmidt, J. E. Hansen, M. J. Menne, A. Persin, R. Ruedy, D. Zyss, Improvements in the GISTEMP Uncertainty Model. *Journal of Geophysical Research: Atmospheres*. **124**, 6307–6326 (2019).
36. M. Zemp, M. Hoelzle, W. Haeberli, Distributed modelling of the regional climatic equilibrium line altitude of glaciers in the European Alps. *Glob Planet Change*. **56**, 83–100 (2007).
37. G. Nigrelli, S. Fratianni, A. Zampollo, L. Turconi, M. Chiarle, The altitudinal temperature lapse rates applied to high elevation rockfalls studies in the Western European Alps. *Theor Appl Climatol*. **131**, 1479–1491 (2018).
38. N. P. Gillett, H. Shiogama, B. Funke, G. Hegerl, R. Knutti, K. Matthes, B. D. Santer, D. Stone, C. Tebaldi, The Detection and Attribution Model Intercomparison Project (DAMIP v1.0) contribution to CMIP6. *Geosci Model Dev*. **9**, 3685–3697 (2016).
39. K. Haustein, M. R. Allen, P. M. Forster, F. E. L. Otto, D. M. Mitchell, H. D. Matthews, D. J. Frame, A real-time Global Warming Index. *Sci Rep*. **7**, 15417 (2017).
40. Global Modeling and Assimilation Office (GMAO), MERRA2 inst1_2d_asm_Nx: 2d, 3-Hourly, Instantaneous, Single-Level, Assimilation, Single-Level Diagnostics (2015), , doi:10.5067/3Z173KIE2TPD.
41. R. A. Rohde, Z. Hausfather, The Berkeley Earth Land/Ocean Temperature Record. *Earth Syst Sci Data*. **12**, 3469–3479 (2020).
42. H. Hersbach, B. Bell, P. Berrisford, S. Hirahara, A. Horányi, J. Muñoz-Sabater, J. Nicolas, C. Peubey, R. Radu, D. Schepers, A. Simmons, C. Soci, S. Abdalla, X. Abellan, G. Balsamo, P. Bechtold, G. Biavati, J. Bidlot, M. Bonavita, G. Chiara, P. Dahlgren, D. Dee, M. Diamantakis, R. Dragani, J. Flemming, R. Forbes, M. Fuentes, A. Geer, L. Haimberger, S. Healy, R. J. Hogan, E. Hólm, M. Janisková, S. Keeley, P. Laloyaux, P. Lopez, C. Lupu, G. Radnoti, P. Rosnay, I. Rozum, F. Vamborg, S. Villaume, J.-N. Thépaut, The ERA5 global reanalysis. *Quarterly Journal of the Royal Meteorological Society*. **146**, 1999–2049 (2020).

43. B. Bell, H. Hersbach, A. Simmons, P. Berrisford, P. Dahlgren, A. Horányi, J. Muñoz-Sabater, J. Nicolas, R. Radu, D. Schepers, C. Soci, S. Villaume, J.-R. Bidlot, L. Haimberger, J. Woollen, C. Buontempo, J.-N. Thépaut, The ERA5 global reanalysis: Preliminary extension to 1950. *Quarterly Journal of the Royal Meteorological Society*. **147**, 4186–4227 (2021).
44. S. Undorf, M. A. Bollasina, G. C. Hegerl, Impacts of the 1900–74 Increase in Anthropogenic Aerosol Emissions from North America and Europe on Eurasian Summer Climate. *J Clim*. **31**, 8381–8399 (2018).
45. L. J. Wilcox, E. J. Highwood, N. J. Dunstone, The influence of anthropogenic aerosol on multi-decadal variations of historical global climate. *Environmental Research Letters*. **8**, 024033 (2013).
46. F. Sera, M. Hashizume, Y. Honda, E. Lavigne, J. Schwartz, A. Zanobetti, A. Tobias, C. Iñiguez, A. M. Vicedo-Cabrera, M. Blangiardo, B. Armstrong, A. Gasparrini, Air Conditioning and Heat-related Mortality: A Multi-country Longitudinal Study. *Epidemiology*. **31**, 779–787 (2020).
47. A. Gasparrini, Y. Guo, M. Hashizume, P. L. Kinney, E. P. Petkova, E. Lavigne, A. Zanobetti, J. D. Schwartz, A. Tobias, M. Leone, S. Tong, Y. Honda, H. Kim, B. G. Armstrong, Temporal Variation in Heat–Mortality Associations: A Multicountry Study. *Environ Health Perspect*. **123**, 1200–1207 (2015).
48. B. Armstrong, F. Sera, A. M. Vicedo-Cabrera, R. Abrutzky, D. O. Åström, M. L. Bell, B. Y. Chen, M. de S. Z. S. Coelho, P. M. Correa, T. N. Dang, M. H. Diaz, D. van Dung, B. Forsberg, P. Goodman, Y. L. L. Guo, Y. Guo, M. Hashizume, Y. Honda, E. Indermitte, C. Íñiguez, H. Kan, H. Kim, J. Kyselý, E. Lavigne, P. Michelozzi, H. Orru, N. V. Ortega, M. Pascal, M. S. Ragettli, P. H. N. Saldiva, J. Schwartz, M. Scortichini, X. Seposo, A. Tobias, S. Tong, A. Urban, C. D. la C. Valencia, A. Zanobetti, A. Zeka, A. Gasparrini, The role of humidity in associations of high temperature with mortality: A multicountry, multicity study. *Environ Health Perspect*. **127**, 097007-1-097007–8 (2019).
49. A. Gasparrini, M. Leone, Attributable risk from distributed lag models. *BMC Med Res Methodol*. **14**, 55 (2014).
50. Q. Zhao, Y. Guo, T. Ye, A. Gasparrini, S. Tong, A. Overcenco, A. Urban, A. Schneider, A. Entezari, A. M. Vicedo-Cabrera, A. Zanobetti, A. Analitis, A. Zeka, A. Tobias, B. Nunes, B. Alahmad, B. Armstrong, B. Forsberg, S.-C. Pan, C. Íñiguez, C. Ameling, C. de la Cruz Valencia, C. Åström, D. Houthuijs, D. van Dung, D. Royé, E. Indermitte, E. Lavigne, F. Mayvaneh, F. Acquaotta, F. De'Donato, F. di Ruscio, F. Sera, G. Carrasco-Escobar, H. Kan, H. Orru, H. Kim, I.-H. Holobaca, J. Kyselý, J. Madureira, J. Schwartz, J. J. K. Jaakkola, K. Katsouyanni, M. Hurtado Diaz, M. S. Ragettli, M. Hashizume, M. Pascal, M. de Sousa Zanotti Stagliorio Coélho, N. Valdés Ortega, N. Ryti, N. Scovronick, P. Michelozzi, P. Matus Correa, P. Goodman, P. H. Nascimento Saldiva, R. Abrutzky, S. Osorio, S. Rao, S. Fratianni, T. N. Dang, V. Colistro, V. Huber, W. Lee, X. Seposo, Y. Honda, Y. L. Guo, M. L. Bell, S. Li, Global, regional, and national burden of mortality associated with non-optimal ambient temperatures from 2000 to 2019: a three-stage modelling study. *Lancet Planet Health*. **5**, e415–e425 (2021).
51. L. Grize, A. Huss, O. Thommen, C. Schindler, C. Braun-Fahrländer, Heat wave 2003 and mortality in Switzerland. *Swiss Med Wkly*. **135**, 200–205 (2005).
52. W. Lee, Y. Kim, F. Sera, A. Gasparrini, R. Park, H. Michelle Choi, K. Prifti, M. L. Bell, R. Abrutzky, Y. Guo, S. Tong, M. de Sousa Zanotti Stagliorio Coelho, P. H. Nascimento Saldiva, E. Lavigne, H. Orru, E. Indermitte, J. J. K. Jaakkola, N. R. I. Ryti, M. Pascal, P. Goodman, A. Zeka, M. Hashizume, Y. Honda, M. Hurtado Diaz, J. César Cruz, A. Overcenco, B. Nunes, J. Madureira, N. Scovronick, F. Acquaotta, A. Tobias, A. M. Vicedo-Cabrera, M. S. Ragettli, Y.-L. L. Guo, B.-Y. Chen, S. Li, B. Armstrong, A. Zanobetti, J. Schwartz, H. Kim, Projections of excess mortality related to diurnal temperature range under climate change scenarios: a multi-country modelling study. *Lancet Planet Health*. **4**, e512–e521 (2020).
53. S. Hempel, K. Frieler, L. Warszawski, J. Schewe, F. Piontek, A trend-preserving bias correction – the ISI-MIP approach. *Earth System Dynamics*. **4**, 219–236 (2013).

Acknowledgments

We are grateful to S. Sippel for valuable advice.

Funding:
Natural Environment Research Council grant NE/S007474/1 (RSS)
Foundation for International Law for the Environment (RSS)
Oxford Martin Programme on the Post-Carbon Transition (RSS)
New Zealand Ministry of Business, Innovation and Employment via the Endeavour Fund (Whakahura program) (LJH)

Author contributions:

Conceptualization: RSS, AMVC, SL, FO, KLE
Methodology: RSS, AMVC, SL, FO, KLE
Investigation: RSS, AMVC, SL
Visualization: AMVC, RSS
Supervision: AMVC, SL, FO, KLE
Writing—original draft: RSS, AMVC
Writing—review & editing: RSS, AMVC, SL, FELO, KB, AH, LJH, JJH, RV, TW, AW, KLE

Competing interests: Include any financial interests of the authors that could be perceived as being a conflict of interest (including but not limited to financial holdings, professional affiliations, advisory positions, and board memberships). Also include any awarded or filed patents pertaining to the results presented in the paper. If the entire group of authors has no competing interests, the authors should declare this (e.g., "Authors declare that they have no competing interests.") In cases where some authors have competing interests and others do not, note the competing interests and then use the following, "All other authors declare they have no competing interests."

Data and materials availability: Temperature observations for Zürich / Fluntern can be downloaded from the KNMI Climate Explorer at http://climexp.knmi.nl/ (last accessed: 19.08.2022). ERA5 reanalysis data are openly available from the Copernicus Climate Change Service at https://cds.climate.copernicus.eu/#!/home (last accessed: 22.04.2022), MERRA2 from NASA Goddard Earth Sciences (GES) Data and Information Services Center (DISC) at https://disc.gsfc.nasa.gov/datasets/M2TMNXSLV_5.12.4/summary (last accessed: 22.04.2022), and Berkeley Earth from http://berkeleyearth.org/data/ (last accessed: 26.08.2022). All the CMIP6 model simulations are obtained from the CEDA Archive-part of NERC's Environmental Data Service at https://catalogue.ceda.ac.uk/?q=CMIP6&sort_by=relevance&results_per_page=20 (last accessed: 25.08.2022).

Mortality data will be made available at the official data repository of the University of Bern (BORIS) on publication.

Code availability: Code for the analysis of climate data will be available upon request to the corresponding author. Code for the epidemiological analysis will be made publicly available on GitHub on publication.

Figures and Tables

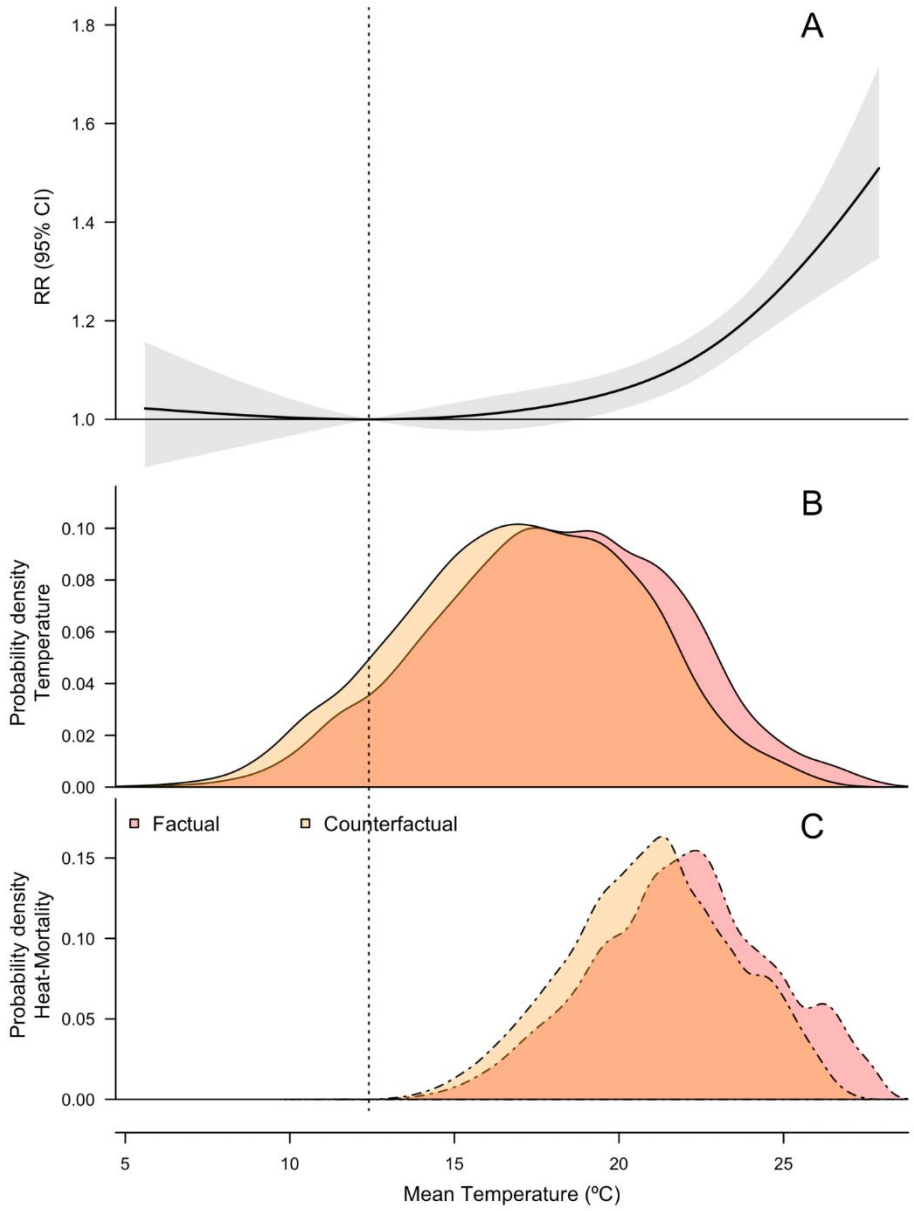

Figure 1: Exposure-response association for the Canton of Zürich, and probability density functions for temperatures under factual and counterfactual conditions, and the resulting distribution of mortality rates. (**A**) exposure-response association calculated using observed temperature and mortality data for 1969-2018, and the 5-95% empirical confidence intervals (shaded area). (**B**) PDFs of observed temperatures and a synthesis of model and observation-based counterfactual temperature timeseries (Methods). (**C**) Proportion of heat-related mortality occurring at different temperatures. The vertical dashed line shows the minimum mortality temperature.

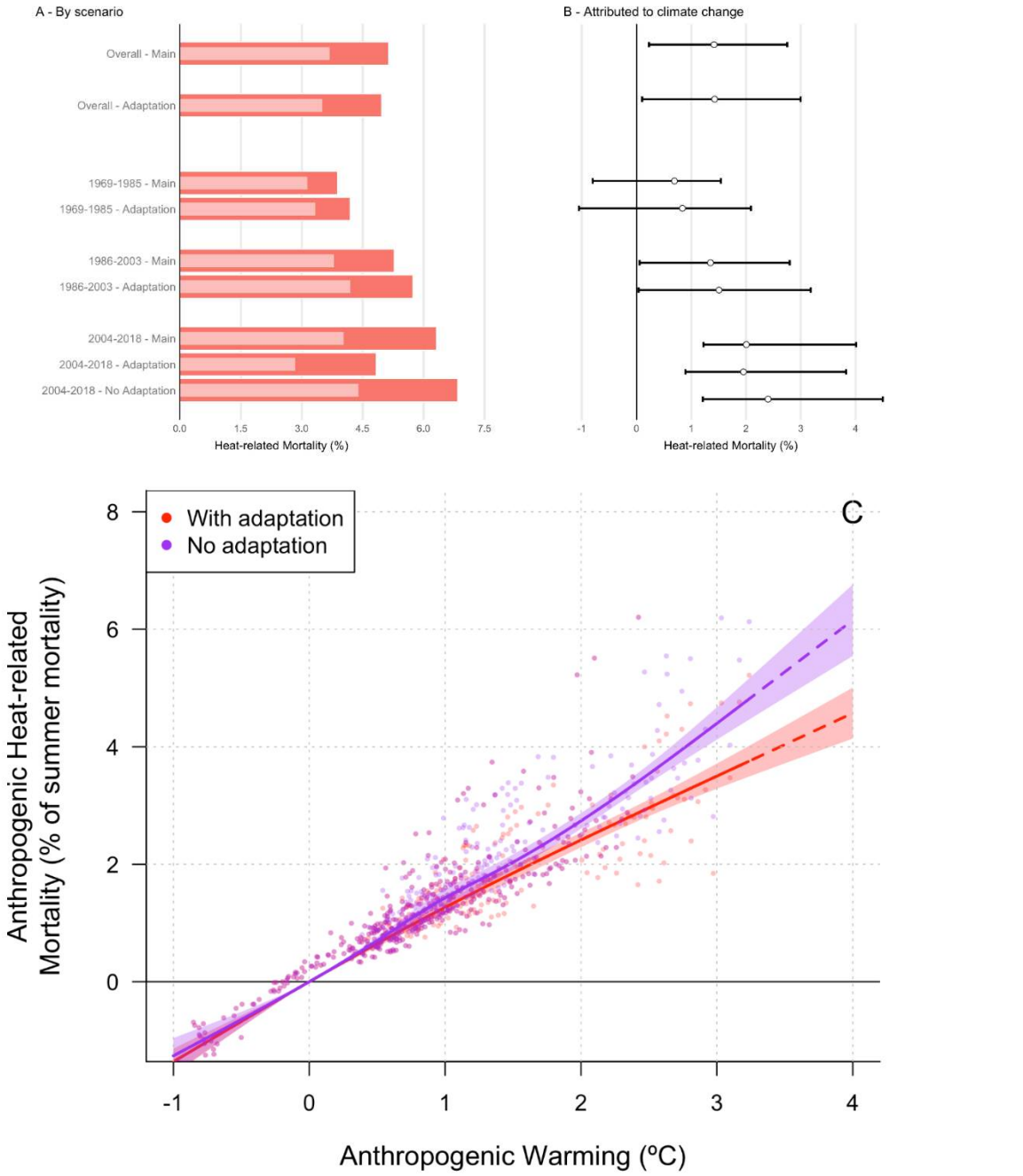

Figure 2: Heat-related mortality attributable to anthropogenic climate change for the Canton of Zürich. (**A**) heat-related mortality as a % of all-cause summer mortality for 1969-2018 (overall exposure-response and 'adaptation' scenario only) and for each of the three time periods considered in the analysis. The 'no-adaptation' and 'adaptation' scenarios were identical for 1969-1985 and 1986-2003 so only 'adaptation' is shown. (**B**) as in panel **A** but showing the heat-related mortality attributable to climate change, with 5-95% empirical confidence intervals. (**C**) the relationship between the regional temperature anomaly attributable to anthropogenic climate change (for Zürich) and the attributable heat-related mortality as a percentage of all-cause summer mortality for the 'adaptation' (red) and 'no-adaptation' scenarios (violet). The trend lines are calculated as a natural spline with 3 degrees of freedom, which produced the best fit to the data of the fits attempted (linear, and natural spline with 3, 4 and 5 degrees of freedom). Dashed lines show the continuation of the fit at temperature anomalies for which no data are available. We note that the 'no-adaptation' scenario only excludes the change in exposure-response

association between 1986-2003 and 2004-2018, and that further adaptation would be expected to occur in response to further warming, reducing the sensitivity of mortality risk to temperature. The shaded area represents the 5-95% confidence intervals of the trend. All values given are the synthesis values of all models and observation-based datasets.

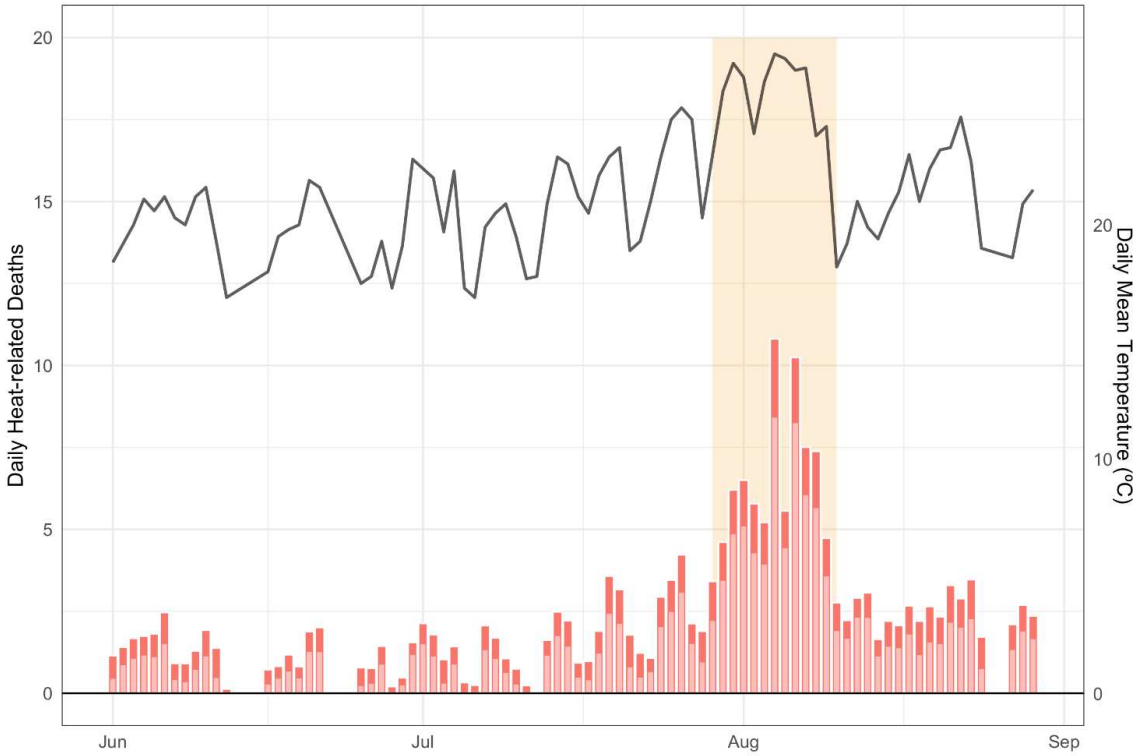

Figure 3: Observed daily-mean temperatures (black) and heat-related mortality (red bars) showing the portion attributable to anthropogenic climate change (dark red) for the Canton of Zürich, June – August 2018. Daily heat-related deaths are represented by the height of the bar, with the dark red segment corresponding to the number of daily deaths attributable to climate change.

Scenario	Mean annual heat-related mortality attributable to anthropogenic climate change		
	1969-1985	1986-2003	2004-2018
Adaptation	19 (-24-48)	38 (1-80)	48 (22-94)
No-adaptation	19 (-24-48)	38 (1-80)	59 (30-110)
Single exposure-response	16 (-18-35)	34 (1-70)	49 (30-98)

Table 1: Mean annual heat-related mortality attributable to anthropogenic climate change for the three periods considered in the analysis and for the three exposure-response scenarios. In the 'adaptation' scenario, a time-varying exposure response association was calculated based on observed temperatures and mortality for each of the three periods. In the 'no-adaptation' scenario, the exposure-response association for 1986-2003 from the 'adaptation' scenario was also used for 2004-2018. In the 'single exposure-response' scenario, the exposure-response association was calculated based on observed mortality and temperature data from the full period (1969-2018). Central estimates and 5-95% confidence intervals were provided for the mortality values.

Supplementary Materials for

Quantifying heat-related mortality attributable to human-induced climate change

Rupert F. Stuart-Smith* *et al.*

*Corresponding author. Email: rupert.stuart-smith@ouce.ox.ac.uk

This PDF file includes:

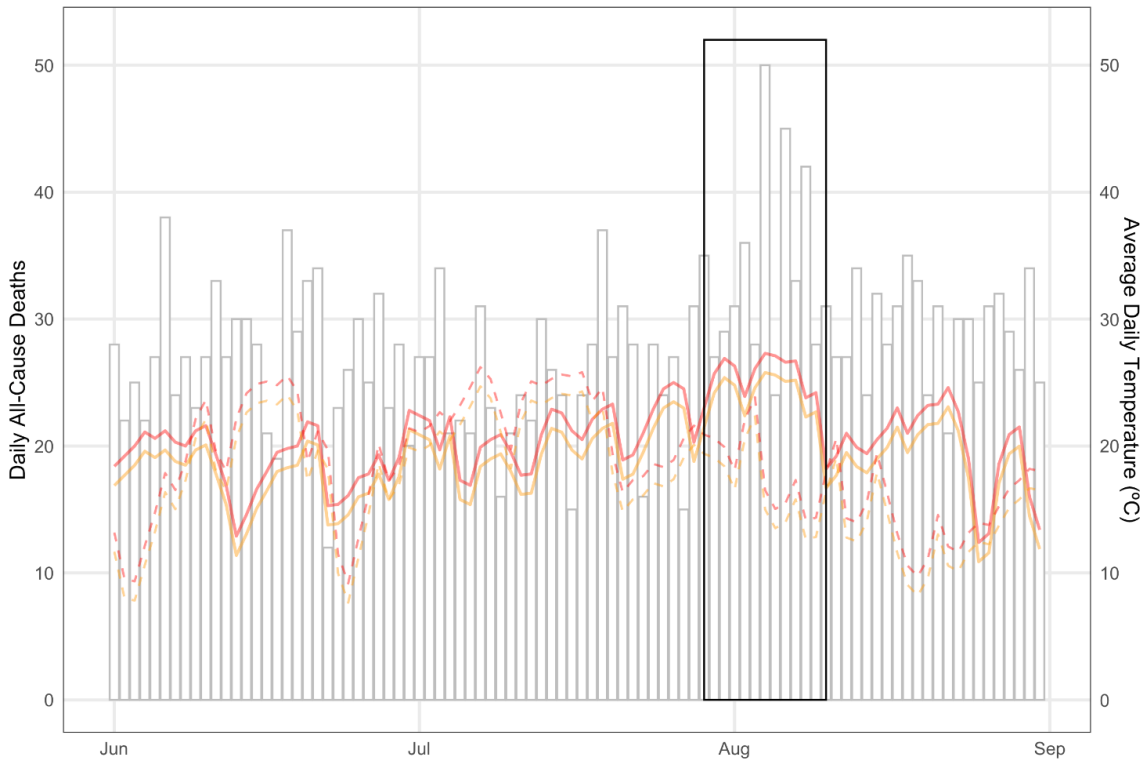

Fig. S1.

Daily all-cause mortality and daily-mean temperatures for the historical (red) and counterfactual (orange) scenarios based on the method applied in this study (solid lines) and the approach taken by Vicedo-Cabrera et al. (2021; dashed lines) (*10*) and for the CMCC-ESM2 model in each case. The dashed lines show historical and historical-natural data from the CMCC-ESM2 model simulations, bias corrected using the same statistical approach (*53*) applied in ref (*10*).

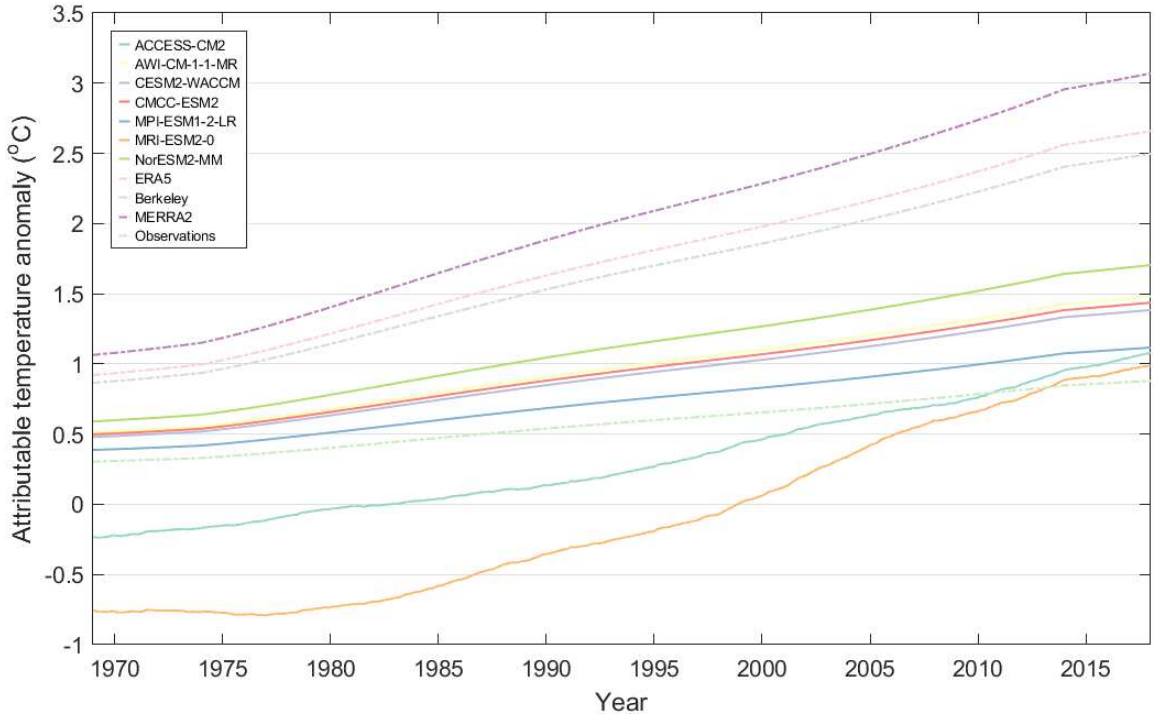

Fig. S2.

Temperature anomaly attributable to anthropogenic climate change for 1969-2018 in climate-model timeseries, reanalysis and station observations. Temperature anomalies are the difference between factual and counterfactual timeseries in each of the observed and model datasets, based on a baseline period of 1989-2018. Observation-based (reanalysis and station records) data are shown as dashed lines, whereas model data are presented as solid lines. The negative anomaly seen in two of the model timeseries during the early portion of the displayed data (ACCESS-CM2 and MRI-ESM2-MM) is explained in Methods ('Constructing the counterfactual temperatures'). By the end of the study period, all models' attributable temperature anomalies lie within the range of the observation-based datasets.

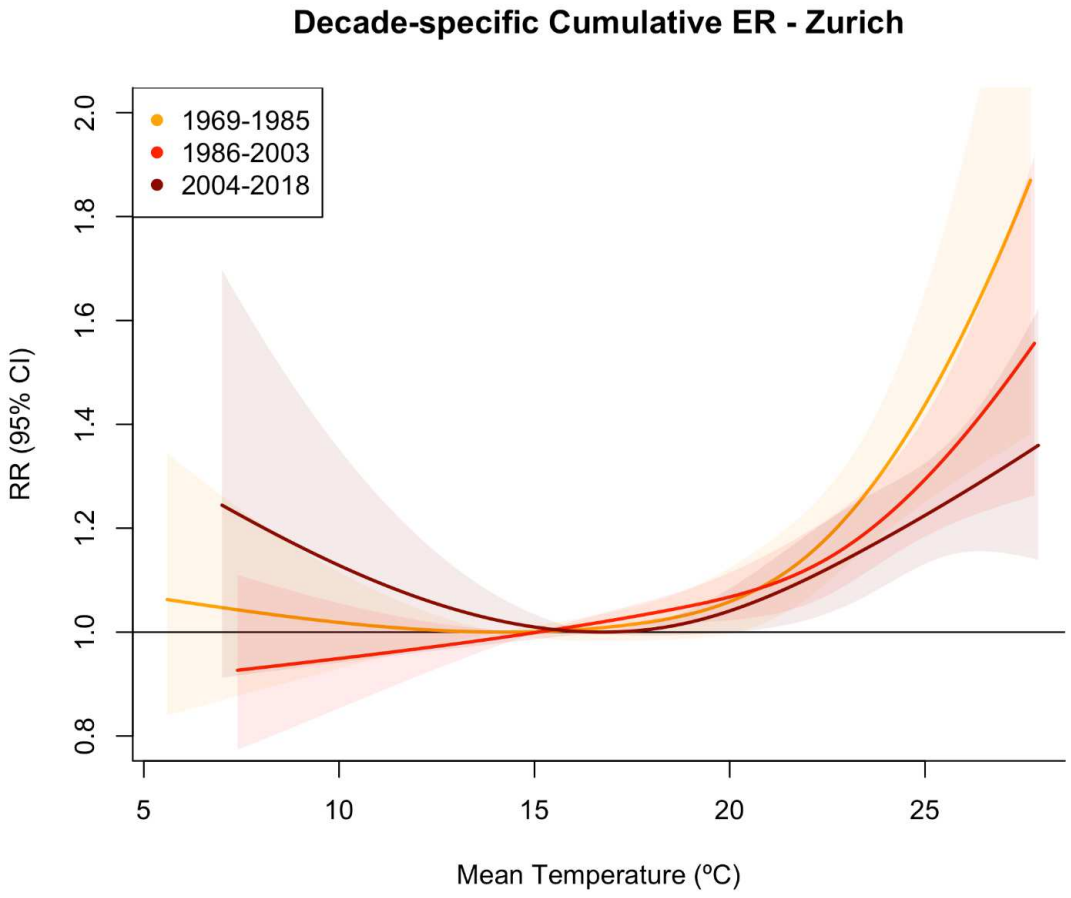

Fig. S3.

Exposure-response associations derived from observed daily-mean temperature and mortality, for 1969-1985, 1986-2003, and 2004-2018. 5-95% empirical confidence intervals are represented by the shaded areas.

Table S1.

CMIP6 models used in analysis showing those selected in the evaluation step and those excluded following evaluation.

Models selected in analysis	Non-selected models
ACCESS.CM2	ACCESS-ESM1-5
AWI-CM-1-1-MR	CESM2
CESM2-WACCM	CEMCC-CM2-SR5
CMCC-ESM2	FGOALS-g3
MPI-ESM1-2-LR	GFDL-ESM4
MRI-ESM2.0	INM-CM4-8
NorESM2-MM	INM-CM5-0
	MIROC6
	MIROC-ES2L
	NorESM2-LM
	TaiESM1

Table S2.

Detailed information for the climate models used for analysis in study.

Climate model	Institute	Spatial resolution (# of grid longitude by latitude)	Experimental ID used
ACCESS-CM2	CSIRO (Commonwealth Scientific and Industrial Research Organisation, Australia), ARCCSS (Australian Research Council Centre of Excellence for Climate System Science)	192 x 144	historical SSP5-8.5 hist-nat
AWI-CM-1-1-MR	Alfred Wegener Institute, Helmholtz Centre for Polar and Marine Research, Germany	384 x 192	historical SSP5-8.5
CESM2-WACCM	National Center for Atmospheric Research, Climate and Global Dynamics Laboratory, USA	288 x 192	historical SSP5-8.5
CMCC-ESM2	Fondazione Centro Euro-Mediterraneo sui Cambiamenti Climatici, Italy	288 x 192	historical SSP5-8.5
MPI-ESM1-2-LR	Max Planck Institute for Meteorology, Alfred WegenerInstitute, Deutsches Klimarechenzentrum and DeutscherWetterdienst, Germany	192 x 96	historical SSP5-8.5
MRI-ESM2-0	Meteorological Research Institute, Tsukuba, Ibaraki 305-0052, Japan	320 x 160	historical SSP5-8.5 hist-nat
NorESM2-MM	NorESM Climate modeling Consortium consists of CICERO, MET-Norway, NERSC, NILU, UiB, UiO and UNI, Norway.	288 x 192	historical SSP5-8.5

Table S3.

Heat-related mortality attributable to anthropogenic climate change for each model and observation-based dataset, 1969-2018.

Dataset (model run or reanalysis)	Central estimate	Confidence interval (lower)	Confidence interval (upper)
ACCESS.CM2	954	761	1140
AWI.CM.1.1.MR	1683	1339	2011
CESM2.WACCM	1585	1262	1893
CMCC.ESM2	1638	1304	1957
MPI.ESM1.2.LR	1306	1042	1555
MRI.ESM2.0	322	178	473
NorESM2.MM	1902	1512	2279
Station observations	1048	835	1243
ERA5	2746	2105	3329
Berkeley Earth	2613	2014	3157
MERRA2	3065	2325	3738
Observations synthesis	2363	914	3548
Model synthesis	1339	253	2104
Full synthesis	1712	276	3329

Table S4.

Fraction of all-cause summer (June-August) mortality attributable to the impact of anthropogenic climate change on temperatures, 1969-2018.

Dataset	Central estimate	Confidence interval (lower)	Confidence interval (upper)
ACCESS.CM2	0.79	0.63	0.94
AWI.CM.1.1.MR	1.39	1.11	1.66
CESM2.WACCM	1.31	1.04	1.57
CMCC.ESM2	1.35	1.08	1.62
MPI.ESM1.2.LR	1.08	0.86	1.29
MRI.ESM2.0	0.27	0.15	0.39
NorESM2.MM	1.57	1.25	1.88
Station observations	0.87	0.69	1.03
ERA5	2.27	1.74	2.75
Berkeley Earth	2.16	1.67	2.61
MERRA2	2.53	1.92	3.09
Observations synthesis	1.95	0.76	2.93
Model synthesis	1.11	0.21	1.74
Full synthesis	1.42	0.23	2.75

Table S5.

Heat-related mortality calculated using the single exposure-response association (derived from all observed temperatures and mortality) and the time-varying exposure-response associations for the 'adaptation' and 'no-adaptation' scenarios. As described in the main text, the exposure-response association calculated for 1986-2003 is also applied to 2004-2018 in the 'no-adaptation' scenario. Bracketed values are the 5-95% empirical confidence intervals.

	Single exposure-response	Adaptation	No-adaptation
Heat-related mortality (historical)	6217 (2825-9623)	6004 (2922-8694)	6742 (3696-9433)
Heat-related mortality (counterfactual)	4457 (1046-8051)	4236 (1618-7273)	4809 (2054-7970)
Attributable heat-related mortality	1712 (276-3329)	1725 (124-3623)	1890 (200-3875)
Heat-related mortality (% of all-cause mortality)	5.1 (2.3-8.0)	5 (2.4-7.2)	5.6 (3.1-7.8)
Counterfactual heat-related mortality (% of all-cause mortality)	3.7 (0.9-6.7)	3.5 (1.3-6.0)	4 (1.7-6.6)
Attributable heat-related mortality (% of all-cause mortality)	1.4 (0.2-2.8)	1.4 (0.1-3.0)	1.6 (0.2-3.2)
Attributable portion of heat-related mortality (%)	27.5	28.7	28

Table S6.

Cumulative 1854-2010 scope 1,2, & 3 emissions attributable to the ten highest-emitting investor- and state-owned companies, the proportion of historical anthropogenic greenhouse gas emissions attributable to these actors, and the estimated heat-related mortality attributable to each company for the Canton of Zürich over 1969-2018. Historical emissions data are sourced from ref. (*30*).

Company	Cumulative emissions 1854-2010 ($GtCO_2e$)	Percent of global anthropogenic emissions (1751-2010)	Attributable heat-related mortality, Zürich 1969-2018
Chevron	51.1	3.52	61
ExxonMobil	46.7	3.22	56
Saudi Aramco	46.0	3.17	55
BP	35.8	2.47	43
Gazprom	32.1	2.22	38
Royal Dutch / Shell	30.8	2.12	37
National Iranian Oil Company	29.1	2.01	35
Pemex	20.0	1.38	24
Conoco Philips	16.9	1.16	20
Petroleos de Venezuela	16.2	1.11	19